

# A Hardware Platform for Tuning of MEMS Devices Using Closed-Loop Frequency Response<sup>1</sup>

Michael I. Ferguson, Jet Propulsion Laboratory, Michael.I.Ferguson@jpl.nasa.gov  
MS 303/300, 4800 Oak Grove Dr., Pasadena, CA 91109, 818-393-6967  
Eric MacDonald – University of Texas at El Paso, emac@utep.edu  
500 West University Dr., El Paso, TX 79968-0523, 915-747-5969  
David Foor – Texas A&M – Kingsville, quatro@ieee.org  
719 W Kleberg, Kingsville, TX 78363, 361-549-6338.

*Abstract*—We report on the development of a hardware platform for integrated tuning and closed-loop operation of MEMS gyroscopes. The platform was developed and tested for the second generation JPL/Boeing Post-Resonator MEMS gyroscope. The control of this device is implemented through a digital design on a Field Programmable Gate Array (FPGA). A software interface allows the user to configure, calibrate, and tune the bias voltages on the microgyro. The interface easily transitions to an embedded solution that allows for the miniaturization of the system to a single chip.

errors in the MEMS devices in order to produce a navigation-grade gyroscope for spaceflight with the form-factor available with these devices. The end result of using the microgyro in these non-conventional environments will reduce size, mass and power while maintaining control of the remote system. Typical applications that would benefit from this technology include: the detection of angular rotation in all axes of a robotic arm, integration of the device in a planetary rover or lunar or planetary sample return missions that have a premium on weight because of the cost of lifting mass off the remote surface.

## TABLE OF CONTENTS

|   |          |
|---|----------|
| <b>1. INTRODUCTION</b> .....                    | <b>1</b> |
| <b>2. MECHANICS OF THE MEMS MICROGYRO</b> ..... | <b>2</b> |
| <b>3. CONTROL OF THE MICROGYRO</b> .....        | <b>2</b> |
| <b>4. GYRO DIGITAL SUBSYSTEM</b> .....          | <b>3</b> |
| <b>5. FUTURE MODIFICATIONS</b> .....            | <b>5</b> |
| <b>6. SUMMARY AND DISCUSSION</b> .....          | <b>5</b> |
| <b>7. ACKNOWLEDGEMENTS</b> .....                | <b>5</b> |
| <b>REFERENCES</b> .....                         | <b>5</b> |
| <b>BIOGRAPHY</b> .....                          | <b>6</b> |

## 1. INTRODUCTION

The JPL/Boeing MEMS gyroscope, or microgyro, is a type of post resonator gyroscope (PRG) that detects the coriolis precession of an oscillating silicon post to determine angular rate of rotation. MEMS PRGs all suffer from degradations in performance due to manufacturing imperfections which errors such as zero-rate drift, or a measured rotation of a stationary gyro. Competing designs such as spinning-mass gyroscopes typically have orders of magnitude higher volume, size and power, so there is a great incentive among the aerospace community to develop lighter, more compact and less power consuming gyroscopes. Other small gyroscope designs have been proposed which measure effects on light passing through a fiber-optic cable [12], however, fibers are notorious for becoming cloudy when exposed to radiation. This adds incentive to correct for the

As a corollary to the advancement of technology, the microgyro suffers, before calibration, from a decrease in accuracy and precision with respect to the larger, spinning-mass types. This is a characteristic passed down by the several parts of the manufacturing process that leads to asymmetry in the silicon structure. This will be explained further in Section 2. The result of the inherent asymmetry results in the existence of a non-degeneracy in the modes of oscillation along the X- and Y-axes. This causes a reduction in the microgyro's sensitivity and zero-rate drift—or the ability of the microgyro to detect no rotation when it is in a static state.

Two general solutions exist for the problem of decreased sensitivity. (1) By increasing the accuracy in the manufacturing process, the microgyro will be more symmetric. This, however, would be expensive and impractical in light of another solution. (2) Corrections can be applied to the system post-fabrication. The corrections are by far more cost effective and take several forms. One option is to apply a transformation to the vibration for both axes of rotation [6]. Unfortunately this method requires a careful characterization of the covariance matrix, which is a numeric measurement of the coupling between the X- and Y-axes. Another method is to adapt the resonant frequency of the gyroscope by applying feedback, a closed-loop approach [5]. A third approach is change the sensing pickoff frame by creating weighted sums of the pickoff signals to decouple the dynamics [1]. The third approach

<sup>1</sup> 0-7803-8155-6/04/\$17.00©2004 IEEE

also allows for a further improvement in the decoupling of the axes by using electrostatic force to modify the spring constants of the vibratory system. As the modes of oscillation become degenerate, sensitivity increases regardless of the device's inherent asymmetry. By calibrating the device to force the case of degenerate oscillation modes, a gyroscope of comparable sensitivity to spinning-mass gyroscopes can be produced.

This paper presents a control system to automatically swap the drive and sense axes in order to extract the resonant frequencies of each axis at a given set of bias voltages. An algorithm can then be applied to iteratively modify the bias voltages. A major advantage of this system is that the resonant frequencies can be extracted quickly (~1 second) as compared with the open-loop control system, which takes two orders of magnitude longer.

This design is realized on an FPGA with augmented portability for future designs and implementations. This paper is organized such that Section 2 describes the mechanics of the microgyro, Section 3 describes the control system, Section 4 describes the Gyro Digital Subsystem, Section 5 describes future directions and Section 6 summarizes the project results.

## 2. MECHANICS OF THE MEMS MICROGYRO

The mechanical design of the microgyro can be seen in Figure 1. There are two posts on the microgyro, one is affixed to the top plate and the other (not shown) is affixed to the baseplate. In order for the gyroscope to operate, the silicon posts (center) must oscillate around an axis (i.e. X as labeled in the figure). Because the oscillations are driven around this axis, it is called the drive axis. Rotation around the Z-axis in the  $\Omega$  direction will cause coriolis forces that couple vibrations from the drive axis to the orthogonal axis, or sense axis. The vibrations coupled to this sense axes are related to the angular rate of rotation. The top post is affixed to four capacitive petals (called a resonator) that are suspended above a micro-machined base plate by four outer silicon springs. The upper and lower plates are set 10 $\mu$ m apart. Oscillations cause a variation of capacitance to occur in the internal structure of the device. This change in capacitance generates a time-varying (sinusoidal) charge that can be converted to a voltage using the relationship,  $V=Q/C$ .

The posts can be driven around the drive axis by applying a time-varying voltage signal to the drive petal electrodes. Because there is symmetry in the device, either of the two axes can be designated as the drive axis. Each axis has a capacitive petal for sensing oscillations as well. The microgyro has additional plates that allow for electro-static damping. Static bias voltages can be used to modify the amount of damping to each oscillation mode. In an ideal, symmetric device, the resonant frequencies of both modes are equal; however, manufacturing imperfections in the

machining of the device can cause dissimilarities in the devices silicon structure. This results in asymmetry of the vibration modes. This can arise from several different places in the fabrication process. One reason asymmetries between the oscillation modes exists is due to imperfect lithography. Because the etching of the silicon is very temperature dependent, imperfect etching can result when temperature gradients form across the silicon wafer. Another reason for the asymmetry is due to the alignment of the top plates to the baseplate. Also, the bonding of the silicon posts can also cause an inconsistency in the modes of oscillation because the posts need to be aligned with respect to the resonator, baseplate and each other. Because of these imperfections, a non-degeneracy in the post's modes of oscillation exists. A resulting split in the resonant frequencies associated with each axis allows the coriolis forces to transfer oscillations from one mode to another inefficiently, and thus, a non-linear relationship between rotation and output voltage is detected. This leaves the microgyro with a 0.1 $^{\circ}$ /hr drift before any electronic calibration. In addition to the resonant frequencies, the two vibration modes induce a second harmonic as well. This harmonic is a cause for the lessened sensitivity of the device. By adjusting the static bias voltages on the capacitor, both harmonics are modified to match each other; this is referred to as the tuning of the device.

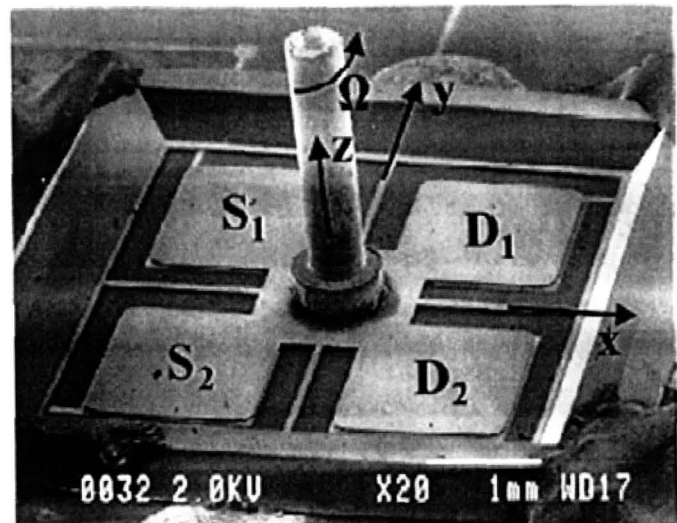


Figure 1. A magnified picture of the JPL microgyro with sense and drive electrodes labeled (picture courtesy of T. Tang, JPL).

## 3. CONTROL OF THE MICROGYRO

As mentioned above, coriolis forces act on the oscillating silicon post causing the plane of oscillation to rotate about the Z-axis. The control system detects this rotation by

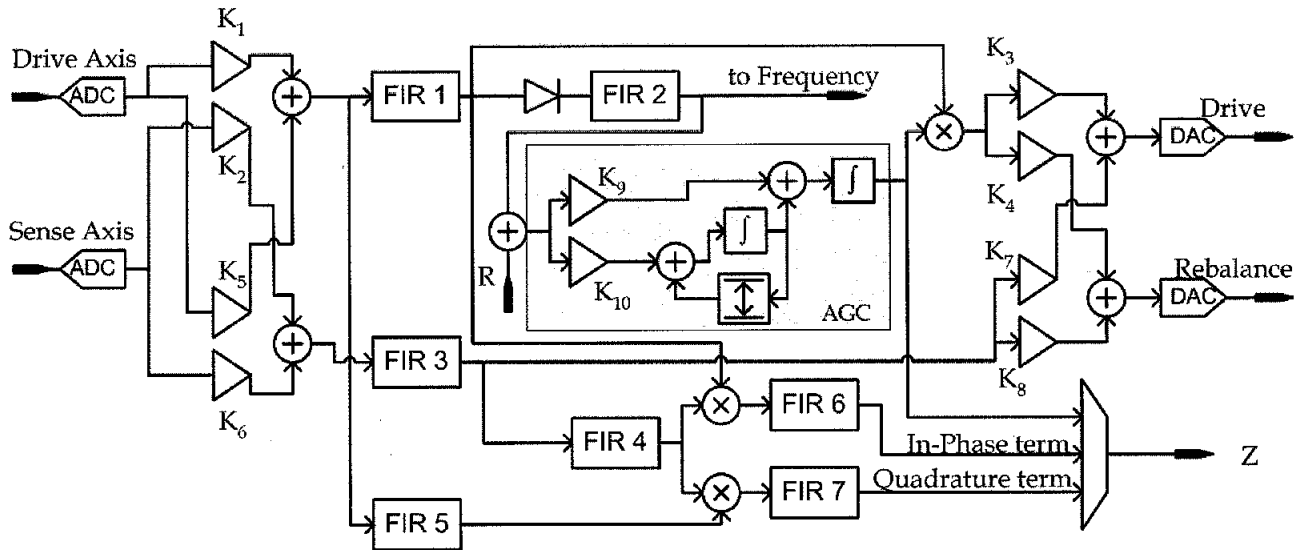


Figure 2. The JPL/Boeing microgyro closed-loop control architecture.

sensing motion around the sense axis. Since the amount of rotation is related to the energy sensed in the “sense” direction, the force required to dampen out that motion is again related to the rotation. This process is called sense rebalancing and the amount of energy dissipated to rebalance is quantified as an amount of angular rotation. If the relationship between the sense and drive axes is non-linear, the resultant energy expelled to rebalance the oscillations will also yield a non-linear quantification of the angular rate. As noted previously, modifying the static bias voltages to cause change the spring constant for both axes allows for a closer linear relationship to exist between the vibration modes. In order to extract the resonant frequencies of the vibration modes, there are two general methods, 1) open-loop and 2) closed-loop control. In an open-loop system, the drive axis is excited with a sine wave at a given frequency and a measurement of the resulting amplitude is made. This is done repeatedly through the frequency spectrum. Because of cross-coupling between the different axes, two peaks will appear, showing the resonant frequencies of both axes. This takes approximately 1.4 minutes to complete and must be done at least three times to average out noise. A faster implementation is a close-loop control whereby the gyro is given an impulse disturbance and allowed to oscillate freely. This so-called “pinging” of the vibration mode allows the gyroscope to immediately settle to its natural frequency. The corresponding frequency, F1, is measured from the sensing plate. Because the device is relatively symmetric, the drive and sense axes are swapped and the other mode is pinged to get F2. The difference in the frequencies is determined very quickly using this technique, about 1.5 seconds, roughly 50 times faster than from the open-loop control method. This ability to quickly swap the drive axis with the sense axis is a feature of the GDS and will be explained in greater detail below.

A diagram of the closed-loop control system can be seen in Figure 2. This circuitry includes a drive loop and a sense

rebalance loop. The drive loop takes the input from the “drive sense” petal (sensory petal along the drive axis), and outputs the forcing signal to the “drive drive” petal electrodes (driving force petal along the drive axis). The sense rebalance loop receives input from the “sense sense” petal (sensory petal along the sense axis), and forces, or rebalances, the oscillations back along the drive axis with a forcing signal to the “sense drive” petal electrode. The magnitude of this forcing function in the rebalance loop is related to the angular rate of rotation. In the figure there are several scaling coefficients indicated  $K_i$ , where  $i$  ranges from 1 to 10. These constants allow for a mixing of the sensed signals from both axes as described in [1]. We augment the use of these constants by using them to swap the meaning of the drive- and sense-axis, so that the bulk of the energy switches between the two, thus allowing the tuning algorithm to measure the resonance frequency along the X- or Y-axis, or indeed any axis between X and Y. A more detailed description of the operation of this control system can be found in [1].

Because the amplitude of the freely oscillating drive axis will naturally decay, another control task is implemented to lightly drive or damp, depending on circumstance, the drive axis so that the amplitude of the driven signal is constant. This feature is implemented through an Automatic Gain Control (AGC) loop, shown shaded in the figure. A signal rectification stage and proportional integrator loop are the main components of the AGC. The output of the AGC is a DC value that modulates the forcing function.

#### 4. GYRO DIGITAL SUBSYSTEM

The system used to implement the control, operation, and observability of the microgyro is referred to as the Gyro Digital Subsystem (GDS). Figure 3 illustrates the closed-

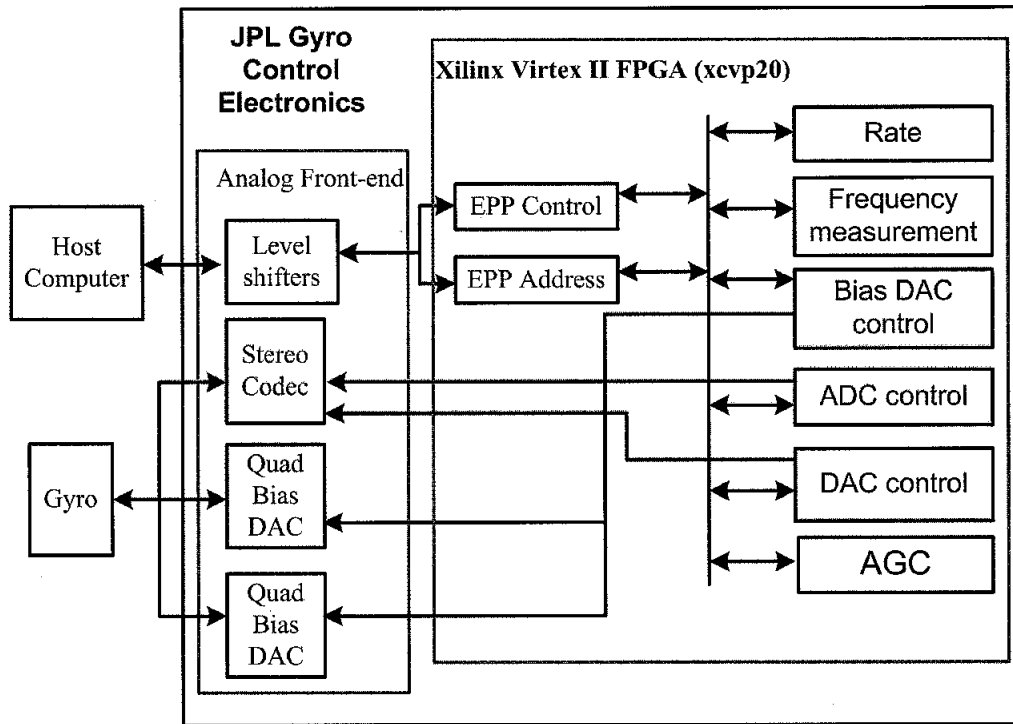


Figure 3. A diagram of the closed-loop control system.

loop control system. The key circuit elements that allow proper operation of the microgyro include the audio codec (Stereo Digital to Analog Converter DAC), high voltage Analog to Digital Converters (ADCs), IEEE-1294 Enhanced Parallel Port (EPP) interface, and the Digital Signal Processor (DSP) functionality.

The audio codec is used to translate the analog signals for both the drive and sense axes for both driving and sensing. Its stereo capabilities allow for two inputs and two outputs. The high-voltage DACs are utilized for the setting of the static bias voltages on the gyroscope, which range from -15V to +60V. The parallel port interface allows for user input/output capabilities. The user can configure the coefficients for the finite impulse response (FIR) filters along with the scaling coefficients (K1 through K8) and PI coefficients ( $K_p$  and  $K_i$ ). The codec is configured through this interface as well.

The AGC design, initially reported by other researchers [1] was improved upon. A graphical user interface (GUI) allows the user to configure the ASIC and codec, change static voltage biases, and monitor outputs from critical areas within the AGC and the output from the demodulation stage, see Figure 2.

The utility of this new control system is realized by the ability to swap the drive signal between the X- and Y-axes for the extraction of the resonant frequencies. As mentioned above, in order to mitigate the mismatch in resonant frequencies the F1 and F2 should be equal. In practice this

is never the case and a maximum error bound must be set in order for this source of error to be effectively removed. The error bound is determined as the point at which the zero-rate drift due to this source of error is zero. This had been determined empirically to be about 0.1Hz [11]. This implementation was tested with a version of the JPL/Boeing Post-Resonator gyroscope with 16 capacitive plates as can be seen in Figure 4. The gyro was operated for a period of several hours and provided a frequency measurement that was stable to 1mHz. A typical capture of the driving and sensed signals for the gyro is seen in Figure 5. In the figure, the signal Torque 2 is the sense-drive or rebalance-drive signal. This signal was observed to be smaller during quiescent operation.

## 6. SUMMARY AND DISCUSSION

The JPL/Boeing microgyro is a device that can be controlled and tuned by implementing an open- or closed-loop control digital system. This paper describes an option for the closed-loop system that has the option of swapping the drive- and sense-axes, thus decreasing the time required for tuning by more than a factor of fifty. Future design modifications will allow for even smaller control circuits by replacing the current 18-bit parallel multipliers and FIR filters by online modules, which routinely reduce the area significantly [2]. Additionally, a future design will include a microprocessor on-chip to allow for in-situ re-tuning of the gyroscope if there is an unexpected change in the behavior due to radiation or other faults. This automated tuning algorithm has been the focus of a parallel research effort [3]. In addition to tuning algorithm, another parallel effort is underway to model the effect of temperature on the performance of the gyroscope [4]. The combination of the intelligent tuning algorithm, a characterization of the temperature dependence and the closed-loop control system will lead to a robust, light-weight, low-power navigation-grade inertial measurement unit for use in space even in the most extreme environments.

## 7. ACKNOWLEDGEMENTS

The work described in this publication was carried out at the Jet Propulsion Laboratory, California Institute of Technology under a contract with the National Aeronautics and Space Administration. Leveraged funding was provided by NASA ESTO-CT, ARDA, and ONR.

## REFERENCES

- [1] Chen, Y. C., M'Closkey, R.T., Tran, T., and Blaes, B., "A control and signal processing integrated circuit for the JPL-Boeing micromachined gyrosopes", to be published, 2004.
- [2] M.D. Ercegovac and T. Lang, *Digital Arithmetic*, Morgan Kaufmann Publishers - An Imprint of Elsevier Science, 2004.
- [3] D. Keymeulen, W. Fink, M. Ferguson, C. Peay, B. Oks, K. Yee, "Tuning of MEMS device using Evolutionary Computation and open-loop Frequency Response Applied to the JPL MEMS microscopic gyro", in Proceedings of the IEEE Aerospace Conference, Big Sky, March 2005.
- [4] M. I. Ferguson, D. Li, "Effect of Temperature on MEMS Vibratory Rate Gyroscope", in Proceedings of the IEEE Aerospace Conference, Big Sky, March 2005

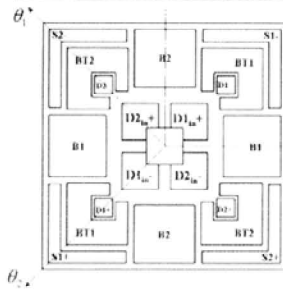
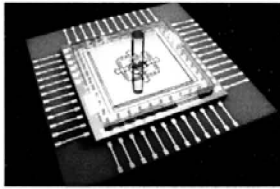


Figure 4. A representative picture of the instrumented MEMS gyro and corresponding diagram of the segmented electrode.

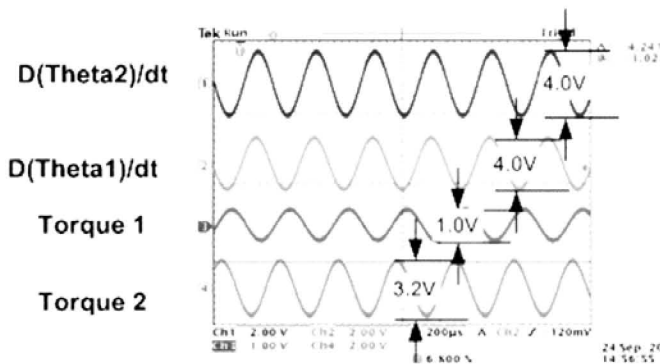


Figure 5. A typical set of waveforms for slight rotation around the Z-axis. The rebalance output can be seen so being approximately 3.2V.

## 5. FUTURE MODIFICATIONS

The existing system currently has a parallel interface to the host computer. This interface is currently being replaced with a serial interface toward the eventual goal of integrating the entire tuning and control package on a single device. In addition to the interface changes, a significant reduction in area, and power will be realized when we replace the 18-bit parallel multipliers and FIR filters currently used with combined units using online arithmetic [2]. This system has not yet been tested in the mode where the drive- and sense-axes are swapped, but based on our previous experiments using electrostatic tuning [3], this will be an effective tool to allow fast tuning of the gyro.

- [5] Leland, R.P., "Adaptive mode tuning for vibrational gyroscopes," IEEE Trans. Control Systems Tech., vol.11, no.2, pp.242–7, March 2003.
- [6] Painter C.C., Shkel A.M., "Active structural error suppression in MEMS vibratory rate integrating gyroscopes," IEEE Sensors Journal, vol.3, no.5, pp.595–606, Oct. 2003.
- [7] R. P. Leland, "Lyapunov based adaptive control of a MEMS gyroscope," in Proc. 2002 Amer. Contr. Conf., Anchorage, AK, 2002, pp. 3765–3770.
- [8] S. Park, "Adaptive control strategies for MEMS gyroscopes," Ph.D. dissertation, Univ. California, Berkeley, 2000.
- [9] S. Park and R. Horowitz, "Adaptive control for Z-axis MEMS gyroscopes," in Proc. American Control Conf., Arlington, VA, June 25–27, 2001, pp. 1223–1228.
- [10] A. M. Shkel, R. Horowitz, A. A. Seshia, S. Park, and R. T. Howe, "Dynamics and control of micromachined gyroscopes," in Proc. American Control Conf., San Diego, CA, June 1999, pp. 2119–2124.
- [11] Discussion with C. Peay.
- [12] Lefevre, H.C., Bourbin Y., Graindorge P., Arditty H.J., "Review of fiber optic gyroscopes", *Proceedings of SPIE the international society for optical engineering* [0277-786X] Lefevre, yr: 1983 vol: 369 pg: 386.

**Eric MacDonald** received a BSEE, MSEE and PhDEE from the University of Texas at Austin in 1992, 1997, and 2002 respectively. He has worked at IBM and Motorola doing circuit and logic design of processors and System-On-Chips (SOC) focusing on testability and ultra-low power design. In 2002, he co-founded a company Pleiades Design and Test, Inc., which was acquired in 2003 by Magma Design Automation, Inc. In 2003, he joined the department of Electrical and Computer Engineering of the University of Texas at El Paso.



**David Foor** is working on his BSEE at Texas A&M – Kingsville. As an undergraduate he received a summer research fellowship through the California Institute of Technology where he interned at the Jet Propulsion Laboratory. He is a member of the IEEE Robotics and Automation Society.



## BIOGRAPHY

**Michael I. Ferguson** is a member of the Technical Staff in the Bio-Inspired Technologies and Systems group. His focus is on evolutionary algorithm application to VLSI design and arithmetic algorithms. He is currently working on the application of GA to tuning MEMS micro gyros. His other projects include evolution of digital and analog circuits intrinsically and extrinsically using a variety of methods. He was the Local Chair of the 2003 NASA/DoD Conference on Evolvable Hardware. He received a M.S. in Computer Science from University of California at Los Angeles and a B.S. in Engineering Physics from the University of Arizona.

